

# Dynamic Nuclear Polarization-Enhanced NMR on Aligned Lipid Bilayers at Ambient Temperature

Orawan Jakdetchai,<sup>†</sup> Vasyi Denysenkov,<sup>‡</sup> Johanna Becker-Baldus,<sup>†</sup> Bercem Dutagaci,<sup>†</sup> Thomas F. Prisner,<sup>‡</sup> and Clemens Glaubitz<sup>\*,†</sup>

<sup>†</sup>Institute of Biophysical Chemistry and <sup>‡</sup>Institute of Physical and Theoretical Chemistry, Center for Biomolecular Magnetic Resonance Frankfurt, Goethe University Frankfurt, 60438 Frankfurt am Main, Germany

**S** Supporting Information

**ABSTRACT:** Dynamic nuclear polarization (DNP)-enhanced solid-state NMR spectroscopy has been shown to hold great potential for functional studies of membrane proteins at low temperatures due to its great sensitivity improvement. There are, however, numerous applications for which experiments at ambient temperature are desirable and which would also benefit from DNP signal enhancement. Here, we demonstrate as a proof of concept that a significant signal increase for lipid bilayers under room-temperature conditions can be achieved by utilizing the Overhauser effect. Experiments were carried out on aligned bilayers at 400 MHz/263 GHz using a stripline structure combined with a Fabry–Perot microwave resonator. A signal enhancement of protons of up to  $-10$  was observed. Our results demonstrate that Overhauser DNP at high field provides efficient polarization transfer within insoluble samples, which is driven by fast local molecular fluctuations. Furthermore, our experimental setup offers an attractive option for DNP-enhanced solid-state NMR on ordered membranes and provides a general perspective toward DNP at ambient temperatures.

Dynamic nuclear polarization (DNP) has emerged as a powerful method to improve the poor sensitivity of NMR and offers a broad range of applications from molecular biophysics via material sciences to magnetic resonance imaging (MRI). The enormous reduction in experimental time by DNP in combination with solid-state NMR (ssNMR) offers new opportunities, e.g., in the areas of membrane proteins or surface chemistry.<sup>1,2</sup> So far, applications of DNP-enhanced ssNMR have mainly relied on combining the well-established cross effect (CE) with magic angle sample spinning (MAS). For these experiments, low temperatures are needed ( $\sim 100$  K) to reach sufficiently long electron relaxation times of the polarizing agents added to the sample. In addition, it is also required to immerse water-containing samples in a glass-forming matrix acting as cryoprotectant and at the same time preventing radical aggregation.<sup>3</sup> The requirement of performing such experiments under cryogenic conditions is especially useful for applications which intrinsically require frozen samples, e.g., for trapping a functionally important protein state or for precise determination of dipole–dipole couplings. These experimental conditions are often associated with line broadening due to freezing-induced disorder and/or para-

magnetic enhancement of transverse relaxation.<sup>4</sup> Therefore, many applications have utilized selective isotope labeling schemes to overcome this problem through reducing spectra complexity.<sup>5,6</sup>

Alternatively to CE, time-dependent fluctuations of the scalar and dipolar couplings between nuclear and electron spins in non-frozen samples result in polarization transfer via the Overhauser effect (OE-DNP).<sup>7</sup> Fluctuations of the hyperfine coupling between the unpaired electron spin of the polarizing agent and the target nuclear spin have to be fast compared to the electron Larmor frequency ( $\omega_e \tau \leq 1$ ), which leads to the conclusion that OE-DNP works best at low magnetic fields. Indeed, numerous applications of OE-DNP at low magnetic field ( $< 1$  T) have been found, including studies of water dynamics<sup>8</sup> and site-specific water accessibility of membrane proteins.<sup>9,10</sup> The OE enhancement,

$$\varepsilon_{\text{OE}} = \frac{\langle I_z \rangle - I_0}{I_0} = \xi f s \frac{\gamma_e}{\gamma_n} \quad (1)$$

depends on the coupling factor  $\xi$  accounting for the cross-relaxation efficiency, the leakage factor  $f$  describing the electronic contributions to the nuclear relaxation, and the saturation factor  $s$  representing the efficiency of microwave (MW) pumping.<sup>11</sup>

Here, we explore OE-DNP as a prospect for polarization enhancement of insoluble molecular complexes such as lipid bilayers under ambient temperature conditions and at a magnetic field of 9.4 T, which is high compared to most OE-DNP applications and which is in the same range as those currently used for CE-DNP. The motivation for this study comes from two different directions: (i) DNP-enhanced ssNMR on non-frozen samples is desirable especially in cases in which highest spectral resolution and/or a fluid bilayer phase is required. (ii) Although OE-DNP has been mainly used at low fields, feasibility studies at higher magnetic fields provided promising proton enhancements of up to  $-80$  for small molecules in the liquid phase.<sup>13,14</sup>

In order to move toward DNP-enhanced ssNMR on non-frozen samples, two experimental challenges have to be addressed: Sample heating due to MW electric field has to be minimized, while at the same time the MW power has to be strong enough to saturate the electron spin transitions. These

Received: October 2, 2014

Published: October 21, 2014

requirements call for a specific experimental setup, in which both radio frequency (RF) and MW frequency are coupled efficiently into the sample in the form of a joint resonance structure. A gyrotron as MW source ensures a sufficiently strong MW field. Unfortunately, due to its mechanical size, a MW resonator is currently not easily integrated into a MAS-NMR probehead. We have therefore turned to “oriented ssNMR” by using thin layers of mechanically aligned lipid bilayers for this proof-of-concept study. The potential use of DNP for oriented ssNMR has been highlighted previously.<sup>15</sup> For this purpose, an almost ideal RF/MW resonance structure is found in the form of a stripline RF probe<sup>16</sup> combined with a Fabry–Perot MW resonator<sup>12</sup> as shown in Figure 1: Thin

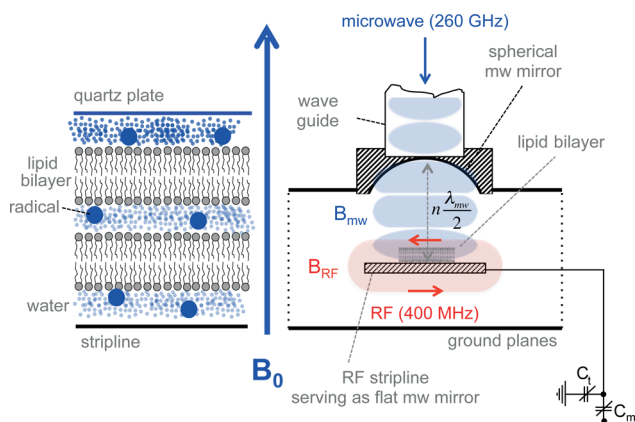


**Figure 1.** Stripline Fabry–Perot probe structure used for DNP-enhanced NMR on fluid lipid membranes at ambient temperature. A thin stack of lipid bilayers is placed on a metal stripline, which creates the  $B_1$ -RF field at the surface and produces the FID. The stripline together with an opposite spherical mirror forms a microwave resonator.<sup>12</sup>

layers of lipid bilayers are aligned on top of the stripline, which generates a strong and homogeneous  $B_1$ -RF field close to the surface, detects the free induction decay (FID), and serves as planar MW mirror within the resonator. The sample thickness is chosen much smaller than the wavelengths of the applied MWs so that heating can be reduced. The stripline probe with Fabry–Perot resonator provides the efficient use of MW power, and a  $Q$ -factor of approximately 100 can be obtained for  $\sim 20$   $\mu\text{m}$  lipid bilayer samples aligned on the stripline.

Lipid bilayers consisting of 1,2-dioleoyl-*sn*-glycero-3-phosphocholine (DOPC) have been aligned within the resonator as shown in Figure 1. The low main-phase transition temperature of DOPC of  $-17$   $^\circ\text{C}$  ensures that the sample is found in the fluid phase under room-temperature conditions. Since the double resonator in its current design only allows  $^1\text{H}$  detection, it had to be verified whether a sufficient spectral resolution of the aligned samples could be achieved. A comparison between  $^1\text{H}$  spectra of DOPC vesicles recorded with and without MAS is shown in Figure 2a. Under MAS, all proton resonances are resolved. Without MAS, lines broaden significantly, but the resonances of the acyl chain and choline protons can still be distinguished from the water signal. This is in contrast to the broad and homogeneous line shapes in “real” solids because the fast anisotropic rotational diffusion of lipids in the fluid phase pre-averages the homonuclear proton dipole–dipole coupling network.

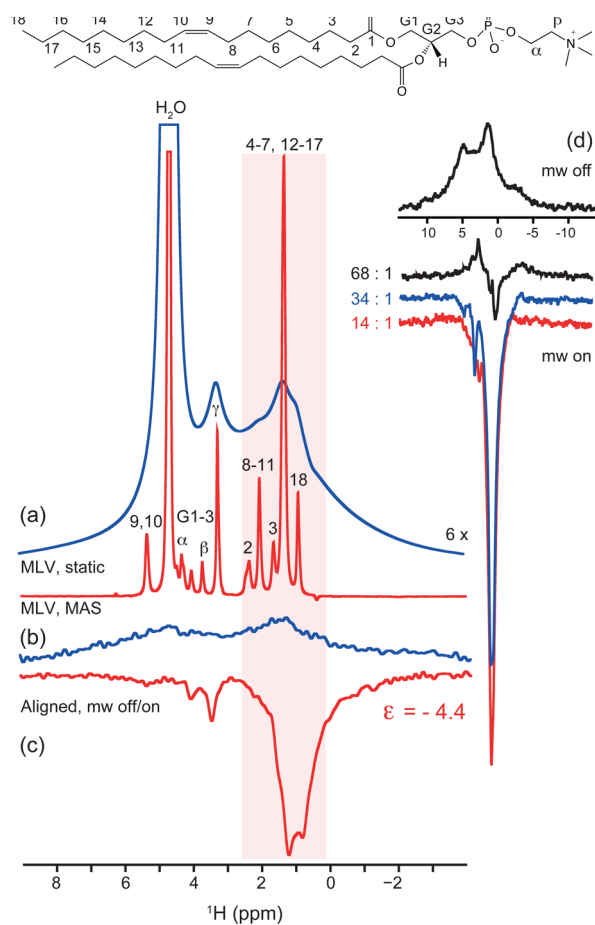


**Figure 2.** (a)  $^1\text{H}$  NMR spectra of DOPC vesicles (static and MAS at 600 MHz). (b)  $^1\text{H}$  NMR spectrum of DOPC aligned as shown in Figure 1, doped with TEMPOL (DOPC:TEMPOL 34:1), and hydrated with  $\text{D}_2\text{O}$  (DOPC: $\text{D}_2\text{O}$  1:27), resulting in a stack of approximately 2000 bilayers of  $20$   $\mu\text{m}$  thickness. (c) Upon microwave irradiation (5.6 W), an enhancement of  $-4.4$  was observed for the acyl chain proton resonances. (d) The enhancement increases with the amount of TEMPOL present.

The separation of lipid and water resonances allows a proof-of-concept study by analyzing whether DNP occurs for water, for lipids, or for both. A stack of approximately 2000 bilayers ( $160$   $\mu\text{g}$ ) was loaded onto the stripline, resulting in a sample diameter of  $3$  mm and thickness of approximately  $20$   $\mu\text{m}$ . DOPC was doped with the monoradical TEMPOL at a molar ratio of 34:1. Under excess hydration and upon irradiation with increasing MW power, a negative DNP enhancement of water can be observed (Figure S1), as previously reported.<sup>8,17</sup> Microwave heating, which is reduced but not completely eliminated by the probehead design, leads to an estimated temperature increase of between  $20$  and  $80$  K, depending on MW power levels, duration of irradiation, and sample amount. However, samples were stable, as the experiments were fully reproducible. For better temperature control, active cooling will be implemented in the next generation of probes.

The hydration level could be safely reduced while keeping the bilayer in the fluid phase to a level of 27:1  $\text{D}_2\text{O}$ :DOPC, so that also the lipid signals could be detected. Under MW irradiation, a strong negative enhancement of the acyl chain but also of the  $\gamma$ -choline protons is observed (Figure 2c). The enhancement generally increases with increasing amount of radical in the membrane (Figure 2d) and also with increasing

MW power (Figure S2). Upon closer inspection of the spectra, it appears that the best enhancement for the acyl chain protons is obtained at the highest tested radical amount, while a DNP effect for the  $\gamma$ -choline resonance is only detected in the presence of less TEMPOL (Figures 2d and S2). One possible explanation could be that TEMPOL, which is hydrophilic, quenches protons at the membrane surface. It is also observed that the overall shape of the DNP-enhanced spectra changes and is slightly narrower compared to the conventional spectra, which could be caused by different DNP enhancement factors experienced by protons at different sites.

In order to verify our findings, experiments were repeated using bilayers consisting of 1,2-dimyristoyl-*sn*-glycero-3-phosphocholine (DMPC). In contrast to DOPC, DMPC has shorter acyl chains without double bonds and features a higher phase transition temperature of 24 °C. Using TEMPOL, an enhancement comparable to that obtained with DOPC was observed (Figure S3). Replacing TEMPOL with biradicals bTbK<sup>18</sup> and TOTAPOL<sup>19</sup> results in larger DNP signals, although the total number of radicals per lipid was kept constant in all three samples. This is surprising, as for OE-DNP in solution, a small-size polarizing agent is usually preferable.<sup>20</sup>

To further characterize the observed DNP effect on lipid bilayers, we have determined the polarization transfer from bTbK to DMPC as a function of  $B_0$  (Figure S4). The largest negative enhancement is observed on the resonance in the middle of the EPR spectrum, where the magnetic field matches the MW frequency.

Our data show unambiguously that a significant DNP enhancement of proton resonances of lipids within stacks of bilayers at reduced hydration, ambient temperature, and high field is possible. The negative DNP enhancement and the shape of the field-dependent enhancement profile (Figure S4) show that the polarization transfer mechanism responsible for our observation is based on the Overhauser effect mediated via electron–nuclei dipole–dipole relaxation. On the other hand, this explanation is not obvious, given that the overall dynamics of radical and target molecule with respect to each other under our experimental conditions (high field, anisotropic system) does not match the  $\omega_e\tau \leq 1$  condition, taking into account that translational diffusion and rotational correlation time are in the order of 30  $\mu\text{m}^2/\text{s}$  and  $1 \times 10^{-10}$  s, respectively.<sup>21</sup> Therefore, the question about the source of efficient dipole–dipole cross-relaxation arises.

As outlined above, OE-DNP depends on the leakage, saturation, and coupling factors. The leakage factor can take values between 0 and 1. Here, for DOPC and TEMPOL, it was found close to 0.7, indicating that electrons contribute approximately 30% to nuclear relaxation (Figure S5). More difficult to determine are saturation factor (which is between 0 and 1) and coupling factor. The latter depends on the molecular dynamics of the nuclei–electron system. For dipolar relaxation, a value between 0 and 0.5 is expected, which decreases with increasing magnetic field. A number of models have been developed to calculate the coupling factor in solution on the basis of rotational and translational motions.<sup>22,23</sup> All of them predict a low DNP enhancement at fields of 9 T and above, which should be even lower in non-soluble systems such as lipid bilayers as studied here.

While we do not yet have an exact model for predicting the coupling factor for our molecular system, it is insightful to consider the molecular dynamics of radical and lipids within the bilayer in more detail. A molecular motion which is fast

compared to the electron Larmor frequency of 263 GHz has a correlation time shorter than 0.6 ps. Characteristic dynamics of lipids in their fluid phase, such as rotational and lateral diffusion, leaflet flip-flops, or undulations, are much slower (Figure S6). For estimating the radical dynamics, we have carried out MD simulations of bTbK within DMPC bilayers. The data show that bTbK equilibrates within the hydrophobic core of the membrane, and the radical center shows fast fluctuations in location and orientation (Figure S7). However, none of these motional modes of lipid and bTbK could account for the dipole–dipole cross-relaxation required to explain the observed OE-DNP effects. However, local motions such as bond rotations/vibrations and trans–gauche isomerizations of the lipid chains are equal to or faster than picoseconds (Figure S6) and could significantly contribute to the relevant relaxation pathways. Indeed, the potential importance of fast local fluctuations for OE-DNP at higher fields had been proposed before.<sup>13,24,25</sup> Since such motions occur universally in biomolecules, optimism seems justified that it might be possible to utilize OE-DNP also for polarizing non-frozen samples of (membrane) proteins.

To further investigate the observed phenomena, the resonator structure used has to be extended with more RF channels, so that <sup>13</sup>C or <sup>15</sup>N detection under <sup>1</sup>H decoupling and MW irradiation will become possible. This will improve the spectral resolution of our aligned samples, which is currently compromised by the residual homonuclear dipole–dipole proton couplings. An improvement in resolution will enable us to analyze whether the observed DNP enhancement is uniform or site-specific, whether hydrophilic or hydrophobic radicals are preferable, and whether our approach can be applied to aligned membrane proteins as well.

OE-DNP effects have also recently been demonstrated in insulating solids.<sup>26</sup> This supports the idea that this polarization mechanism is more widely applicable at higher fields and also offers a general perspective toward DNP of non-frozen but non-soluble samples.

## ■ ASSOCIATED CONTENT

### 📄 Supporting Information

Materials and Methods section, OE-DNP on water in aligned bilayers (Figure S1), OE-DNP as a function of microwave power and radical concentration (Figure S2), OE-DNP on DMPC with mono- and biradicals (Figure S3), field-dependent enhancements profile (Figure S4), determination of the leakage factor (Figure S5), and time scales and MD simulations for radicals in lipid bilayers (Figures S6 and S7). This material is available free of charge via the Internet at <http://pubs.acs.org>.

## ■ AUTHOR INFORMATION

### Corresponding Author

glaubitz@em.uni-frankfurt.de

### Notes

The authors declare no competing financial interest.

## ■ ACKNOWLEDGMENTS

This work was supported by the Deutsche Forschungsgemeinschaft (GL 307/4-1). We are grateful to Dr. Jörn Plackmeier, Frankfurt, for synthesizing TOTAPOL and to Dr. Olivier Ouari and Prof. Paul Tordo, Aix Marseille Université, for kindly providing bTbK.

## ■ REFERENCES

- (1) Ni, Q. Z.; Daviso, E.; Can, T. V.; Markhasin, E.; Jawla, S. K.; Swager, T. M.; Temkin, R. J.; Herzfeld, J.; Griffin, R. G. *Acc. Chem. Res.* **2013**, *46*, 1933.
- (2) Rossini, A. J.; Zagdoun, A.; Lelli, M.; Lesage, A.; Coperet, C.; Emsley, L. *Acc. Chem. Res.* **2013**, *46*, 1942.
- (3) Zagdoun, A.; Casano, G.; Ouari, O.; Schwarzwald, M.; Rossini, A. J.; Aussenac, F.; Yulikov, M.; Jeschke, G.; Coperet, C.; Lesage, A.; Tordo, P.; Emsley, L. *J. Am. Chem. Soc.* **2013**, *135*, 12790.
- (4) Koers, E. J.; van der Crujisen, E. A.; Rosay, M.; Weingarth, M.; Prokofyev, A.; Sauvee, C.; Ouari, O.; van der Zwan, J.; Pongs, O.; Tordo, P.; Maas, W. E.; Baldus, M. *J. Biomol. NMR* **2014**, DOI: 10.1007/s10858-014-9865-8.
- (5) Ong, Y. S.; Lakatos, A.; Becker-Baldus, J.; Pos, K. M.; Glaubitz, C. *J. Am. Chem. Soc.* **2013**, *135*, 15754.
- (6) Bajaj, V. S.; Mak-Jurkauskas, M. L.; Belenky, M.; Herzfeld, J.; Griffin, R. G. *Proc. Natl. Acad. Sci. U.S.A.* **2009**, *106*, 9244.
- (7) Overhauser, A. W. *Phys. Rev.* **1953**, *91*, 476.
- (8) Kausik, R.; Han, S. *Phys. Chem. Chem. Phys.* **2011**, *13*, 7732.
- (9) Cheng, C. Y.; Han, S. *Annu. Rev. Phys. Chem.* **2013**, *64*, 507.
- (10) Doll, A.; Bordignon, E.; Joseph, B.; Tschaggelar, R.; Jeschke, G. *J. Magn. Reson.* **2012**, *222*, 34.
- (11) Hausser, K. H.; Stehlik, D. In *Advances in Magnetic and Optical Resonance*; Waugh, J. S., Ed.; Academic Press: New York, 1968; Vol. 3, p 79.
- (12) Denysenkov, V.; Prisner, T. *J. Magn. Reson.* **2012**, *217*, 1.
- (13) Neugebauer, P.; Kruppenacker, J. G.; Denysenkov, V. P.; Parigi, G.; Luchinat, C.; Prisner, T. F. *Phys. Chem. Chem. Phys.* **2013**, *15*, 6049.
- (14) Prandolini, M. J.; Denysenkov, V. P.; Gafurov, M.; Endeward, B.; Prisner, T. F. *J. Am. Chem. Soc.* **2009**, *131*, 6090.
- (15) Salnikov, E. S.; Ouari, O.; Koers, E.; Sarrouj, H.; Franks, T.; Rosay, M.; Pawsey, S.; Reiter, C.; Bandara, P.; Oschkinat, H.; Tordo, P.; Engelke, F.; Bechinger, B. *Appl. Magn. Reson.* **2012**, *43*, 91.
- (16) van Bentum, P. J. M.; Janssen, J. W. G.; Kentgens, A. P. M.; Bart, J.; Gardeniers, J. G. E. *J. Magn. Reson.* **2007**, *189*, 104.
- (17) Denysenkov, V.; Prandolini, M. J.; Gafurov, M.; Sezer, D.; Endeward, B.; Prisner, T. F. *Phys. Chem. Chem. Phys.* **2010**, *12*, 5786.
- (18) Matsuki, Y.; Maly, T.; Ouari, O.; Karoui, H.; Le Moigne, F.; Rizzato, E.; Lyubenova, S.; Herzfeld, J.; Prisner, T.; Tordo, P.; Griffin, R. G. *Angew. Chem., Int. Ed.* **2009**, *48*, 4996.
- (19) Song, C.; Hu, K. N.; Joo, C. G.; Swager, T. M.; Griffin, R. G. *J. Am. Chem. Soc.* **2006**, *128*, 11385.
- (20) Hofer, P.; Parigi, G.; Luchinat, C.; Carl, P.; Guthausen, G.; Reese, M.; Carlomagno, T.; Griesinger, C.; Bennati, M. *J. Am. Chem. Soc.* **2008**, *130*, 3254.
- (21) Marsh, D. *Handbook of lipid bilayers*, 2nd ed.; CRC Press, Taylor & Francis Group: Boca Raton, FL, 2013.
- (22) Sezer, D. *Phys. Chem. Chem. Phys.* **2014**, *16*, 1022.
- (23) Sezer, D.; Prandolini, M. J.; Prisner, T. F. *Phys. Chem. Chem. Phys.* **2009**, *11*, 6626.
- (24) Griesinger, C.; Bennati, M.; Vieth, H. M.; Luchinat, C.; Parigi, G.; Hofer, P.; Engelke, F.; Glaser, S. J.; Denysenkov, V.; Prisner, T. F. *Prog. Nucl. Magn. Reson. Spectrosc.* **2012**, *64*, 4.
- (25) Jeschke, G. *Prog. Nucl. Magn. Reson. Spectrosc.* **2013**, *72*, 42.
- (26) Can, T. V.; Caporini, M. A.; Mentink-Vigier, F.; Corzilius, B.; Walish, J. J.; Rosay, M.; Maas, W. E.; Baldus, M.; Vega, S.; Swager, T. M.; Griffin, R. G. *J. Chem. Phys.* **2014**, *141*, 064202.